Research in Astron. Astrophys. **2012** Vol. **12** No. **4**, 419–432
http://www.raa-journal.org *http://www.iop.org/journals/raa*

***R**esearch in*
***A**stronomy and*
***A**strophysics*

A new photometric study of the triple star system EF Draconis *

Yuan-Gui Yang

School of Physics and Electronic Information, Huaibei Normal University, Huaibei 235000, China; *yygcn@163.com*
Key Laboratory of the Structure and Evolution of Celestial Objects, Chinese Academy of Sciences, Kunming 650011, China

Received 2011 November 6; accepted 2012 January 4

Abstract We present new charge-coupled device (CCD) photometry for the triple star EF Draconis, obtained in 2009 and 2011. Using the updated Wilson-Devinney program, the photometric solutions were deduced from two sets of light curves. The results indicate that EF Dra is an A-type W UMa binary with a contact degree of $f = 46.7\%(\pm 0.6\%)$ and a third light of $l_3 \simeq 1.5\%$. Through analyzing the $O - C$ curve, it is found that the orbital period shows a long-time increase with a light-time orbit. The period, semi-amplitude and eccentricity of the third body are $P_{\rm mod} = 17.20(\pm 0.18)\,{\rm yr}$, $A = 0.0039^{\rm d}(\pm 0.0002^{\rm d})$ and $e = 0.49(\pm 0.02)$ respectively. This kind of tertiary companion may extract angular momentum from the central system. The orbital period of EF Dra secularly increases at a rate of $dP/dt = +3.72(\pm 0.07) \times 10^{-7}\ {\rm d\ yr^{-1}}$, which may be interpreted by mass transfer from the less massive to the more massive component. As period increases, the separation between components may increase, which will cause the contact degree to decrease. With mass transferring, the spin angular momentum will increase, while the orbital angular momentum will decrease. Only if the contact configuration would merge at $J_{\rm spin} > \frac{1}{3} J_{\rm orb}$ could this kind of deep-contact binary with period increasing, such as EF Dra, evolve into a rapidly-rotating single star.

Key words: stars (including multiple): binaries: close — stars: individual (EF Draconis)

1 INTRODUCTION

Formation of binaries is a fascinating subject (Zinnecker & Mathieu 2001). The difficulties of this complex process have been recently reviewed by many authors (i.e. Kondo et al. 2002; Tohline 2002; Bate 2004). Studies of close binary stars can provide some key information for the thermal relaxation oscillation and angular momentum loss (e.g., Robertson & Eggleton 1977). Most close binary stars exist in multiple systems, although this hypothesis may be further confirmed by observations and statistical investigations.

Table 1 tabulates 35 contact triple or multiple binaries, including their spectroscopic parameters, which are observed at the David Dunlap Observatory (DDO). This kind of additional companion may remove angular momentum from the central system via Kozai oscillation (Kozai 1962) or a

* Supported by the National Natural Science Foundation of China.

Table 1 Spectroscopic Orbital Elements for Some Tertiary or Quadruple components of W UMa-type Binaries

No.	Star Name	Spectral	$q_{\rm sp}$	Period (d)	$(M_1+M_2)\sin^3 i$	Ref.
1	BD+7°3142	K2V	0.662(8)	0.275277	1.050(14)	[1]
2	V410 Aur	G0/2V	0.144(13)	0.366340	1.42(10)	[2]
3	44i Boo	K2V	0.487(6)	0.267818	1.132(11)	[3]
4	EL Boo	K1/2V	0.248(7)	0.413772	1.448(28)	[4]
5	TZ Boo	F/G5	0.207(5)	0.297160	1.118(18)	[4]
6	EE Cet	F8V	0.315(5)	0.379917	1.706(41)	[5]
7	KR Com	G0IV	0.091(2)	0.407968	0.517(8)	[5]
8	V401 Cyg	F0V	0.290(11)	0.582714	2.008(130)	[5]
9	EF Dra	F8/9V	0.160(14)	0.424000	1.970(124)	[6]
10	CT Eri	F2/3V	0.30(9)	0.634200	–	[7]
11	V345 Gem	F7V	0.142(3)	0.274769	1.054(13)	[8]
12	V899 Her	F5	0.566(18)	0.421173	2.331(77)	[3]
13	SZ Hor	F3V	0.47(4)	0.625118	–	[7]
14	CE Hyi	F5V	–	0.4408	–	[9]
15	VZ Lib	G0	0.237(68)	0.358263	1.704(120)	[3]
16	AM Leo	F5V	0.459(4)	0.365799	1.882(12)	[8]
17	XY Leo	K0V	0.729(7)	0.284098	1.188(12)	[8]
18	VW LMi	F5V	0.416(4)	0.477550	2.282(18)	[10]
19	DE Oct	A9IV	–	0.555592	–	[9]
20	V2388 Oph	F3V	0.186(2)	0.802298	1.926(20)	[5]
21	V2610 Oph	F8/G2V	0.291(9)	0.426512	1.441(31)	[4]
22	ER Ori	F7/8	0.656(12)	0.423403	2.285(45)	[11]
23	V1387 Ori	A4V	0.165(5)	0.730166	0.969(16)	[4]
24	V592 Per	F2IV	0.408(7)	0.715722	2.521(72)	[12]
25	HI Pup	F6V	0.19(6)	0.432616	–	[7]
26	Y Sex	F5/6	0.195(8)	0.419820	1.663(45)	[11]
27	II UMa	F5III	0.172(4)	0.825220	2.180(80)	[5]
28	FT UMa	K0V	0.984(19)	0.654704	2.077(10)	[4]
29	HX UMa	F4V	0.291(9)	0.379156	0.775(30)	[2]
30	TU UMi	F2	0.16(7)	0.377088	0.65(27)	[11]
31	TV UMi	F8V	0.739(21)	0.415549	0.879(12)	[10]
32	AG Vir	A5V	0.382(21)	0.642651	2.563(41)	[10]
33	HT Vir	F8V	0.812(8)	0.407670	2.285(38)	[3]
34	PY Vir	K1/2V	0.773(5)	0.311251	1.387(10)	[1]
35	GSC 1387–0475	K3/5V	0.474(8)	0.217811	0.288(8)	[13]

Notes: The values of $(M_1+M_2)\sin^3 i$ are in solar mass units, while the period is in days. The standard errors in the table are expressed in units of the last decimal places quoted, which are given in parentheses after each value.

Reference: [1] Rucinski et al. (2008); [2] Rucinski et al. (2003); [3] Rucinski et al. (2001); [4] Pribulla et al. (2009b); [5] Rucinski et al. (2002); [6] Lu & Rucinski (1999); [7] Duerbeck & Rucinski (2007); [8] Pribulla et al. (2007); [9] Rucinski & Duerbeck (2006); [10] Pribulla et al. (2006); [11] Pribulla et al. (2009a); [12] Rucinski et al. (2005); [13] Rucinski & Pribulla (2008).

combination of the Kozai cycle and tidal friction (e.g., Fabrycky & Tremaine 2007). Therefore, this will result in a low angular momentum remnant in the close binary.

EF Dra ($= 1E1806.1 + 6944$) was discovered as an X-ray source in the *Einstein Observatory* Extended Medium Sensitivity Survey (Gioia et al. 1987). Based on X-ray observations and three radial velocity measurements, Fleming et al. (1989) suggested that it is a W UMa-type binary, with a distance of $d = 153.5$ pc and a soft-X-ray flux of $f_{\rm X} = 1.38$. They also gave its spectral type as F9, which was recently revised to be F8/9V (Pribulla et al. 2009a). Robb & Scarfe (1989) published VRI observations with large scatter and improved the period value to $0.42400^{\rm d}$. Kazarovets & Samus (1990) designated it as EF Dra and cataloged it as an EW/KW-type binary. Plewa et al. (1991) obtained incomplete light curves and derived a mass ratio of $q_{\rm ph} = 0.125$. Wunder & Agerer

(1992) also photoelectrically observed this star and revised its period to be 0.42402394^{d}. Pribulla et al. (2001a) published BV light curves of EF Dra and determined its absolute parameters. The orbital inclination and fill-out factor are $i = 78.13°(\pm 0.33°)$ and $f = 45.5\%(\pm 2.3\%)$, respectively. Based on 35 light minimum times only spanning $11\ \mathrm{yr}$, they derived a parabolic ephemeris superimposed by a light time orbit, whose period and amplitude are $P_3 = 1360(\pm 150)\ \mathrm{d}$ and $A = 0.002^{\mathrm{d}}$, respectively. Alternatively, they pointed out that the orbital period increase may be a part of a light time orbit due to another companion with a period of at least $12\ \mathrm{yr}$. Therefore, one cannot decide which case is true due to the small number of observations with large scatters. Based on 43 spectra observed in 1991 and 1992, Lu (1993) concluded that EF Dra is a triple star system. Then Lu & Rucinski (1999) published 16 high dispersion spectra. The radial velocity of $-38\ \mathrm{km\,s^{-1}}$ for the third companion is very close to the systemic velocity of $-42\ \mathrm{km\,s^{-1}}$ for the eclipsing pair. Therefore, EF Dra with a physical companion is an A-type W UMa star with an extremely low mass ratio of $q_{\mathrm{sp}} = 0.160(\pm 0.014)$. Due to the extremely low mass ratio and high fill-out factor, the triple star system EF Dra was included in our observing program in order to study the nature of period changes and its evolutionary status.

2 OBSERVATIONS AND REDUCTIONS

The multicolor photometry of the binary EF Dra was carried out using the 60-cm telescope in 2009 and the 85-cm telescope (Zhou et al. 2009) in 2011 at the Xinglong Station of National Astronomical Observatories of China (NAOC). Both telescopes were equipped with the standard Johnson-Cousin-Bessel $UBVR_cI_c$ systems. Image reductions were done using the Image Reduction (IMRED) and Aperture Photometry (APPHOT) packages in the Image Reduction and Analysis Facility (IRAF) in a standard fashion.

On 2009 September 12 and 28, and October 13, EF Dra were observed using the 60-cm telescope. In the field of EF Dra, the nearest star GSC 4433–0827 (10.6^{m} in the V band) has been identified to be a multi-periodic δ Scuti star (Yang et al. 2011). Fainter comparison and check stars (i.e. C1 and Ch1) were chosen, and are listed in Table 2. Typical exposure times for BVR bands were 45 s, 30 s and 20 s. We obtained a total of 403, 444 and 407 images in BVR bands. The light curves (i.e. LC_1) are displayed in the left panel of Figure 1, where there exists a short gap near the secondary eclipse. The phases were computed with a period of 0.42403^{d} (Kreiner 2004). The mean differences between the magnitude of the check star and that of the comparison one are very large,

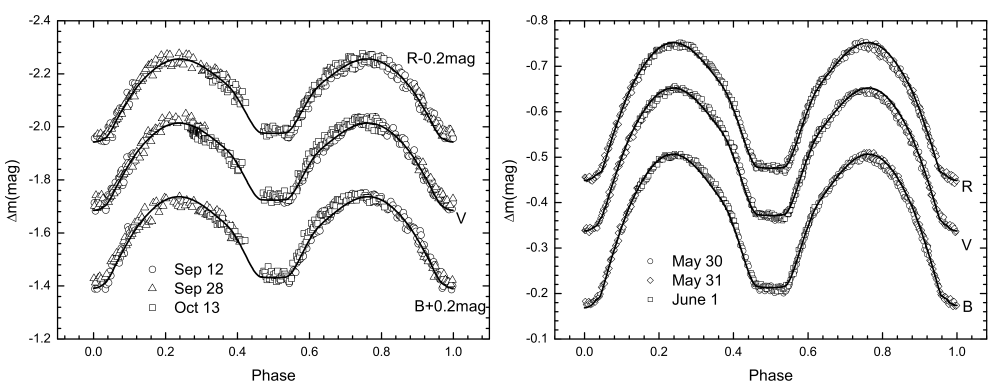

Fig. 1 BVR light curves of the eclipsing binary EF Dra, observed in 2009 (*left panel*) and 2011 (*right panel*). The solid lines were constructed by new photometric solutions.

Table 2 Coordinates of the Variable, Comparison Stars and Check Stars

Star	$\alpha_{\rm J2000.0}$	$\delta_{\rm J2000.0}$	mag (V)	Telescope
EF Dra	18:05:30.35	+69:45:15.4	10.6	
C1	18:06:08.52	+69:43:42.6	12.5	60-cm
C2	18:04:22.68	+69:52:47.7	11.2	85-cm
Ch1	18:06:53.70	+69:45:35.7	12.5	60-cm
Ch2	18:05:07.36	+69:55:22.2	12.0	85-cm

up to $0.01^{\rm m}$, which may result from the faint comparison star because the nearest star GSC 4433–0827 is identified to be variable. Using the 85-cm telescope at the Xinglong station of NAOC, we again observed this binary on three consecutive nights of 2011 May 30 and 31, and June 1. Another two stars were used as the comparison and check stars (i.e. C2 and Ch2), whose coordinates are also listed in Table 2. The exposure times were adopted to be $20\,{\rm s}$, $15\,{\rm s}$ and $10\,{\rm s}$ for BVR bands, respectively. A set of complete light curves (i.e. $\rm LC_2$), including 565, 564 and 548 observations in BVR bands, is shown in the right panel of Figure 1. The precisions of individual points do not exceed $0.005^{\rm m}$. All observations of two sets of light curves, i.e. the magnitude differences in the sense of the variable minus the comparison star together with their heliocentric Julian dates, are available upon request. From Figure 1, EF Dra is an A-type total eclipsing binary, with a duration of totality being about 50 minutes. The primary eclipse is deeper than the secondary eclipse by up to $0.02^{\rm m}$. The amplitudes of variable light are $0.33^{\rm m}$, $0.31^{\rm m}$ and $0.30^{\rm m}$ for BVR bands respectively, which agree with the value of $\Delta V \approx 0.32^{\rm m}$ (Robb & Scarfe 1989). Moreover, EF Dra was observed for other nights in 2009 and 2011 in order to measure its eclipse times. From the new observations, ten light minimum timings were determined by the K-W method (Kwee & van Woerden 1956). Those individual light minimum times, together with their errors, are listed in Table 3.

3 ANALYSIS OF PERIOD CHANGES

Based on a 12-year eclipsing cycle of EF Dra, Pribulla et al. (2001a) suggested that there exists a light-time orbit with a period of $P_3 \approx 3.5\,{\rm yr}$ or $P_3 > 12\,{\rm yr}$. In order to study orbital period changes, we collected a total of 93 light minimum times (5 visual, 50 photoelectric, 38 CCD measurements).

Table 4 tabulates those compiled eclipsing times. In Col. (3) of this table, “vi,” “pe” and “CCD” refer to visual observations, photoelectric measurements, and charge-coupled device, respectively. According to various measurement precisions, weights of 1 and 10 are assigned to visual, and photoelectric or CCD measurements, respectively. Using the linear ephemeris (Kreiner 2004),

$$\text{Min.I} = \text{HJD } 2452500.3076 + 0.42403 \times E, \tag{1}$$

we can calculate the residuals of $(O-C)_1$ for all light minimum times, which are listed in Col. (6) of Table 4, and are displayed in Figure 2.

The general trend of the $(O-C)_1$ curve can be obviously described by an upward parabolic curve, indicating that the orbital period may be increasing. In the calculation process, weights 1 and 10 are assigned to visual, and photoelectric or CCD measurements, respectively. A linear fitting method yielded the following quadratic ephemeris,

$$\text{Min.I} = \text{HJD } 2452500.3086(2) + 0.42402945(3) \times E + 3.16(4) \times 10^{-10} \times E^2, \tag{2}$$

where the parentheses contain the standard errors in units of the last decimal place. Equation (2) is plotted in Figure 2 as a solid line. With the coefficient of the quadratic term, a continuous period increase rate of $dP/dt = +3.72(\pm 0.07) \times 10^{-7}\ {\rm d\ yr^{-1}}$ ($+3.22(\pm0.06)\ {\rm s\ century^{-1}}$) can be obtained. The computed residuals of $(O-C)_2$ are listed in Col. (7) of Table 4. The $(O-C)_2$ curve is shown in the upper section of top panel of Figure 3, whose shape appears to have a quasi-sinusoidal

Table 3 New Obtained Light Minimum Times of EF Dra

JD (Hel.)	Error	Min.	Filter	Telescope
2455087.32057	±0.00050	I	B	60-cm
2455087.32033	±0.00057	I	V	60-cm
2455087.32032	±0.00064	I	R	60-cm
2455103.00713	±0.00052	I	B	60-cm
2455103.01080	±0.00059	I	V	60-cm
2455103.01116	±0.00045	I	R	60-cm
2455118.06499	±0.00099	II	B	60-cm
2455118.06542	±0.00123	II	V	60-cm
2455118.06587	±0.00129	II	R	60-cm
2455165.98809	±0.00103	II	B	60-cm
2455165.98378	±0.00070	II	V	60-cm
2455165.98665	±0.00080	II	R	60-cm
2455675.24953	±0.00033	II	B	85-cm
2455675.25148	±0.00034	II	V	85-cm
2455675.25180	±0.00036	II	R	85-cm
2455678.21810	±0.00030	II	B	85-cm
2455678.21799	±0.00025	II	V	85-cm
2455678.21812	±0.00029	II	R	85-cm
2455709.17140	±0.00005	II	B	85-cm
2455709.17384	±0.00062	II	V	85-cm
2455709.17334	±0.00058	II	R	85-cm
2455712.14253	±0.00026	II	B	85-cm
2455712.14241	±0.00023	II	V	85-cm
2455712.14211	±0.00029	II	R	85-cm
2455713.20105	±0.00013	I	B	85-cm
2455713.20110	±0.00012	I	V	85-cm
2455713.20118	±0.00016	I	R	85-cm
2455714.26222	±0.00049	II	B	85-cm
2455714.26186	±0.00061	II	V	85-cm
2455714.26180	±0.00058	II	R	85-cm

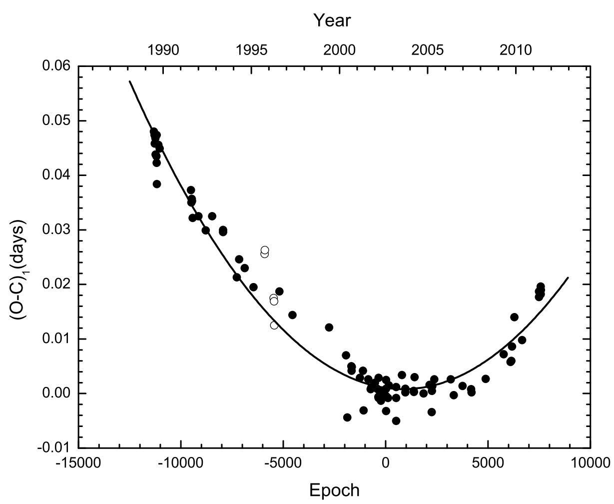

Fig. 2 $(O-C)_1$ diagram of EF Dra. The open and filled circles refer to visual observations, and photoelectric and CCD measurements, respectively. The solid line was constructed by Eq. (2).

Table 4 All Available Times of Light Minimum for EF Dra

JD (Hel.)	Method	Epoch	Min	$(O-C)_1$	$(O-C)_2$	$(O-C)_3$	Ref.
2447701.8201	pe	−11316.5	II	+0.0480	+0.0003	+0.0019	[1]
2447701.8201	pe	−11316.5	II	+0.0480	+0.0003	+0.0019	[1]
2447715.8125	pe	−11283.5	II	+0.0474	+0.0000	+0.0016	[1]
2447716.8710	pe	−11281.0	I	+0.0458	−0.0016	+0.0000	[1]
2447727.8971	pe	−11255.0	I	+0.0472	+0.0000	+0.0016	[1]
2447730.8650	pe	−11248.0	I	+0.0468	−0.0003	+0.0013	[1]
2447734.8902	pe	−11238.5	II	+0.0438	−0.0033	−0.0017	[1]
2447752.4872	pe	−11197.0	I	+0.0435	−0.0032	−0.0016	[2]
2447759.4876	pe	−11180.5	II	+0.0474	+0.0008	+0.0024	[2]
2447760.3305	pe	−11178.5	II	+0.0423	−0.0043	−0.0027	[2]
2447763.5069	pe	−11171.0	I	+0.0384	−0.0081	−0.0065	[2]
2447792.3481	pe	−11103.0	I	+0.0456	−0.0004	+0.0012	[2]
2447820.3334	pe	−11037.0	I	+0.0449	−0.0006	+0.0009	[2]
2448467.3956	pe	−9511.0	I	+0.0373	+0.0025	+0.0029	[3]
2448475.4498	pe	−9492.0	I	+0.0350	+0.0003	+0.0006	[4]
2448488.3835	pe	−9461.5	II	+0.0357	+0.0012	+0.0015	[4]
2448491.5633	pe	−9454.0	I	+0.0353	+0.0009	+0.0012	[4]
2448502.3729	pe	−9428.5	II	+0.0322	−0.0021	−0.0018	[3]
2448624.2819	pe	−9141.0	I	+0.0325	+0.0001	+0.0001	[3]
2448775.4460	pe	−8784.5	II	+0.0299	−0.0003	−0.0008	[3]
2448909.4420	pe	−8468.5	II	+0.0325	+0.0042	+0.0033	[3]
2449132.4789	pe	−7942.5	II	+0.0296	+0.0043	+0.0026	[5]
2449132.4793	pe	−7942.5	II	+0.0300	+0.0047	+0.0030	[6]
2449416.5707	pe	−7272.5	II	+0.0213	−0.0004	−0.0033	[7]
2449465.5495	pe	−7157.0	I	+0.0246	+0.0035	+0.0004	[7]
2449580.4600	pe	−6886.0	I	+0.0230	+0.0032	−0.0004	[8]
2449763.6375	pe	−6454.0	I	+0.0195	+0.0018	−0.0027	[9]
2449995.3760	vi	−5907.5	II	+0.0256	+0.0103	+0.0048	[9]
2449999.4050	vi	−5898.0	I	+0.0263	+0.0111	+0.0055	[9]
2450180.4570	vi	−5471.0	I	+0.0175	+0.0040	−0.0020	[9]
2450189.5730	vi	−5449.5	II	+0.0169	+0.0035	−0.0025	[9]
2450195.5050	vi	−5435.5	II	+0.0125	−0.0008	−0.0068	[9]
2450301.5187	pe	−5185.5	II	+0.0187	+0.0063	+0.0003	[10]
2450571.4095	pe	−4549.0	I	+0.0144	+0.0043	−0.0010	[11]
2451331.4810	pe	−2756.5	II	+0.0121	+0.0072	+0.0049	[12]
2451680.4526	pe	−1933.5	II	+0.0070	+0.0037	+0.0026	[13]
2451705.4590	CCD	−1874.5	II	−0.0044	−0.0076	−0.0087	[14]
2451789.4263	pe	−1676.5	II	+0.0050	+0.0022	+0.0014	[15]
2451796.4220	pe	−1660.0	I	+0.0042	+0.0014	+0.0006	[15]
2451798.3308	pe	−1655.5	II	+0.0049	+0.0021	+0.0013	[15]
2451968.5769	pe	−1254.0	I	+0.0029	+0.0007	+0.0004	[16]
2452031.3346	pe	−1106.0	I	+0.0042	+0.0022	+0.0021	[17]
2452041.5040	CCD	−1082.0	I	−0.0031	−0.0051	−0.0052	[18]
2452139.4607	pe	−851.0	I	+0.0026	+0.0009	+0.0011	[17]
2452189.2824	pe	−733.5	II	+0.0008	−0.0008	−0.0005	[17]
2452203.2757	pe	−700.5	II	+0.0011	−0.0005	−0.0002	[17]
2452252.2516	pe	−585.0	I	+0.0016	+0.0001	+0.0006	[17]
2452277.6938	CCD	−525.0	I	+0.0020	+0.0006	+0.0011	[19]
2452321.5799	pe	−421.5	II	+0.0009	−0.0004	+0.0002	[17]
2452348.5043	CCD	−358.0	I	−0.0006	−0.0019	−0.0012	[17]
2452352.3203	CCD	−349.0	I	−0.0008	−0.0021	−0.0014	[17]
2452352.5360	CCD	−348.5	II	+0.0029	+0.0016	+0.0023	[17]
2452369.4948	CCD	−308.5	II	+0.0005	−0.0007	+0.0000	[20]
2452401.5073	pe	−233.0	I	−0.0013	−0.0025	−0.0017	[17]
2452415.5014	CCD	−200.0	I	−0.0002	−0.0014	−0.0006	[21]
2452509.4210	pe	+21.5	II	−0.0032	−0.0042	−0.0032	[22]
2452510.4852	pe	+24.0	I	+0.0009	−0.0001	+0.0009	[22]
2452511.3349	pe	+26.0	I	+0.0025	+0.0015	+0.0025	[22]
2452511.5439	pe	+26.5	II	−0.0005	−0.0015	−0.0005	[22]

Table 4 — *Continued.*

JD (Hel.)	Method	Epoch	Min	$(O-C)_1$	$(O-C)_2$	$(O-C)_3$	Ref.
2452550.3423	pe	+118.0	I	−0.0008	−0.0018	−0.0007	[17]
2452568.3659	CCD	+160.5	II	+0.0015	+0.0005	+0.0016	[23]
2452717.4122	CCD	+512.0	I	+0.0012	+0.0004	+0.0017	[23]
2452717.6180	CCD	+512.5	II	−0.0050	−0.0058	−0.0045	[23]
2452718.4702	CCD	+514.5	II	−0.0008	−0.0016	−0.0003	[20]
2452835.5067	CCD	+790.5	II	+0.0034	+0.0026	+0.0040	[24]
2452908.4374	CCD	+962.5	II	+0.0009	+0.0001	+0.0016	[25]
2452909.4968	CCD	+965.0	I	+0.0002	−0.0006	+0.0009	[25]
2453082.5013	pe	+1373.0	I	+0.0005	−0.0004	+0.0012	[25]
2453084.4092	CCD	+1377.5	II	+0.0003	−0.0006	+0.0010	[25]
2453098.4049	CCD	+1410.5	II	+0.0030	+0.0021	+0.0037	[25]
2453285.3991	pe	+1851.5	II	+0.0000	−0.0011	+0.0006	[25]
2453410.2776	CCD	+2146.0	I	+0.0016	+0.0003	+0.0021	[26]
2453452.4636	pe	+2245.5	II	−0.0034	−0.0048	−0.0030	[25]
2453458.6159	CCD	+2260.0	I	+0.0005	−0.0009	+0.0009	[14]
2453466.4614	pe	+2278.5	II	+0.0014	+0.0000	+0.0018	[25]
2453507.8055	CCD	+2376.0	I	+0.0026	+0.0011	+0.0029	[27]
2453848.5136	CCD	+3179.5	II	+0.0026	+0.0001	+0.0018	[28]
2453911.4791	CCD	+3328.0	I	−0.0003	−0.0030	−0.0013	[28]
2454091.6936	CCD	+3753.0	I	+0.0014	−0.0020	−0.0005	[14]
2454270.4216	CCD	+4174.5	II	+0.0008	−0.0035	−0.0022	[14]
2454279.5377	CCD	+4196.0	I	+0.0002	−0.0041	−0.0028	[14]
2454570.4248	CCD	+4882.0	I	+0.0027	−0.0032	−0.0024	[29]
2454943.5757	CCD	+5762.0	I	+0.0072	−0.0012	−0.0013	[30]
2455087.3204	CCD	+6101.0	I	+0.0058	−0.0037	−0.0043	[31]
2455103.0097	CCD	+6138.0	I	+0.0060	−0.0036	−0.0042	[31]
2455118.0654	CCD	+6173.5	II	+0.0086	−0.0011	−0.0018	[31]
2455165.9862	CCD	+6286.5	II	+0.0140	+0.0039	+0.0031	[31]
2455327.7494	CCD	+6668.0	I	+0.0098	−0.0017	−0.0030	[32]
2455675.2509	CCD	+7487.5	II	+0.0187	+0.0040	+0.0013	[31]
2455678.2181	CCD	+7494.5	II	+0.0177	+0.0030	+0.0002	[31]
2455709.1729	CCD	+7567.5	II	+0.0183	+0.0033	+0.0004	[31]
2455712.1424	CCD	+7574.5	II	+0.0196	+0.0046	+0.0017	[31]
2455713.2011	CCD	+7577.0	I	+0.0182	+0.0032	+0.0003	[31]
2455714.2620	CCD	+7579.5	II	+0.0190	+0.0039	+0.0010	[31]

Notes: [1] Robb & Scarfe (1989); (2) Plewa et al. (1991); [3] Wunder & Agerer (1992); [4] Hübscher et al. (1992); [5] Hübscher et al. (1993); [6] Hübscher et al. (1994); [7] Agerer & Hübscher (1995); [8] Agerer & Hübscher (1996); [9] Molik (2007); [10] Agerer & Hüebscher (1997); [11] Agerer & Hübscher (1999); [12] Agerer et al. (2001); [13] Agerer & Hübscher (2002); [14] Brát et al. (2007); [15] Pribulla et al. (2001a); [16] Pribulla et al. (2001b); [17] Pribulla et al. (2002); [18] Diethelm (2001); [19] Sarounova & Wolf (2005); [20] Agerer & Hübscher (2003); [21] Diethelm (2002); [22] Drozdz & Ogloza (2005); [23] Diethelm (2003); [24] Hübscher (2005); [25] Pribulla et al. (2005); [26] Zejda et al. (2006); [27] Nelson (2006); [28] Parimucha et al. (2007); [29] Borkovits et al. (2008); [30] Hübscher et al. (2010); [31] Present work; [32] Diethelm (2010).

variation, i.e. a light-time orbit (Irwin 1952), which is more flexible than a sinusoidal one. In order to search for the period of oscillation, Fourier analysis was carried out for the residuals of $(O-C)_2$, whose result is displayed in the bottom panel of Figure 3. We found a significant peak in the power spectrum mainly located around the frequency of $f_1 = 1.6225 \times 10^{-4}\ \mathrm{d}^{-1}$, which corresponds to a period of $6160\ \mathrm{d}$ ($\sim 17\ \mathrm{yr}$). The Levenberg−Marquardt technique (Press et al. 1992) was applied in the calculation process. A nonlinear least-squares fitting method led to the following equation,

$$O-C = -0.0020(\pm 0.0002) + A \times \left(\frac{1-e^2}{1+e\cos\nu} + e\sin\omega\right), \tag{3}$$

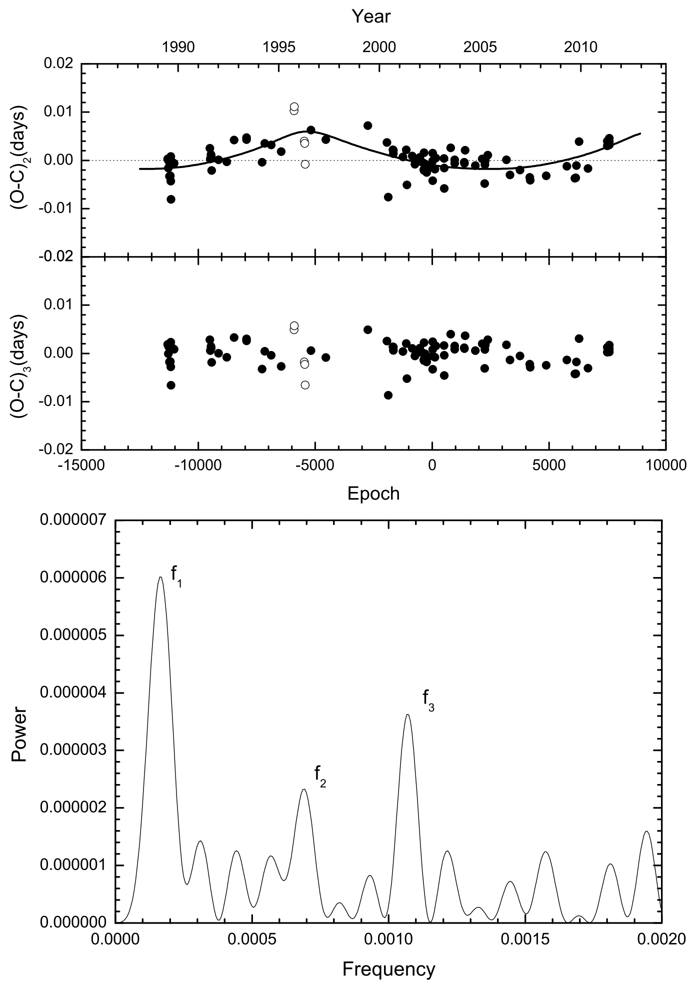

Fig. 3 *Top panel*: the $(O-C)_2$ curve (*upper*) and corresponding curve of residuals $(O-C)_3$ (*lower*). The solid line represents the light-time orbit in Eq. (3). Other symbols are the same as in Fig. 2. *Bottom panel*: the power spectrum of the residuals $(O-C)_2$.

where $A = a_{12} \sin i/c$ is the semi-amplitude, and other parameters are taken from Irwin (1952). The fitted parameters are listed as follows: $A = 0.0039^{\rm d}$ $(\pm 0.0002^{\rm d})$, $P_{\rm mod} = 17.20(\pm 0.18)\,{\rm yr}$, $e = 0.49(\pm 0.02)$, $\omega = 1.4064(\pm 0.0209)$ and T_p = HJD24501665(± 65). The derived period is consistent with one of the predicted values (i.e. $P_3 > 15\,{\rm yr}$; Pribulla et al. 2001a). The solid line is constructed by Equation (3) in the upper section of top panel of Figure 3. The corresponding residuals of $(O-C)_3$, listed in Col. (8) of Table 4, are also shown in its lower section of top panel. From this figure, no regularity is apparent although there exists a bit of scatter.

4 LIGHT-CURVE SOLUTION

Two sets of multi-color light curves for EF Dra (LC_1 in 2009 and LC_2 in 2011) were applied to derive the photometric solution using the W-D code (Wilson & Devinney 1971), including the Kurucz (1993) stellar atmosphere model and a detailed reflection treatment (Wilson 1990). During the calculation, Mode 3 (i.e. the contact configuration) was always used. We adopted a set of fixed parameters (q, T_1, $A_{1,2}$, $g_{1,2}$, $X_{1,2}$ and $Y_{1,2}$, $x_{1,2}$ and $y_{1,2}$), while other parameters (i, T_2, Ω_1, L_1, and L_3) were adjustable in the range of commonly used values.

The spectroscopic elements for the triple star EF Dra were published by Lu & Rucinski (1999). The mass ratio was fixed at $q_{\rm sp} = 0.16$ and the third light L_3 was adjusted. The mean effective temperature of Star 1 was adopted to be $T_1 = 6250$ K based on the spectral type of F8V (Pribulla et al. 2009a). Following Lucy (1967) and Ruciński (1973), gravity darkening exponents of $g_{1,2} = 0.32$ and bolometric albedo coefficients of $A_{1,2} = 0.5$ were set, which are appropriate for stars with convective envelopes. According to the effective temperatures of both components, the logarithmic bolometric (X and Y) and monochromatic (x and y) limb-darkening coefficients were interpolated from the tables in van Hamme (1993). After some iterations, the photometric solutions can be deduced from $\rm LC_1$ and $\rm LC_2$, whose results are listed in Table 5 where two sets of parameters are in agreement. The contributions of the third light to the total light ($l_3 \simeq 1.7\%$ in 2009 and $l_3 \simeq 1.45\%$ in 2011) are much smaller than the value of $l_3 \simeq 0.14$ (Pribulla et al. 2001a). The corresponding theoretical light curves were shown as solid lines in both panels of Figure 1. The value of $\Sigma(O-C)_i^2$ is 0.2817 for $\rm LC_1$, which is larger than that of 0.2624 for $\rm LC_2$. Therefore, we accepted Sol.2 (i.e. $\rm LC_2$ in 2011) as the final solution. The contact degree of $f = 46.7\%(\pm0.6\%)$ approximately agrees with that of $f = 45.5\%(\pm2.3\%)$ (Pribulla et al. 2001a), indicating that EF Dra is a deep-contact triple star system.

Table 5 Photometric Solutions of the Triple Star System EF Dra

Parameter	Sol.1 ($\rm LC_1$ in 2009)	Sol.2 ($\rm LC_2$ in 2011)
$i(^\circ)$	$78.0(\pm0.5)$	$77.8(\pm0.2)$
$q = M_2/M_1$	0.16	
T_1(K)	6250	
T_2(K)	$6299(\pm20)$	$6186(\pm7)$
$\Omega_1 = \Omega_2$	$2.0790(\pm0.0047)$	$2.0818(\pm0.0014)$
f	$49.5\%(\pm2.3\%)$	$46.7\%(\pm0.6\%)$
$L_{1B}/(L_{1B}+L_{2B})$	$0.8207(\pm0.0292)$	$0.8368(\pm0.0101)$
$L_{1V}/(L_{1V}+L_{2V})$	$0.8235(\pm0.0269)$	$0.8356(\pm0.0091)$
$L_{1R}/(L_{1R}+L_{2R})$	$0.8248(\pm0.0261)$	$0.8347(\pm0.0084)$
L_{3B}	$1.73\%(\pm0.15\%)$	$1.45\%(\pm0.05\%)$
L_{3V}	$1.69\%(\pm0.14\%)$	$1.48\%(\pm0.05\%)$
L_{3R}	$1.69\%(\pm0.14\%)$	$1.43\%(\pm0.04\%)$
r_1(pole)	$0.5163(\pm0.0012)$	$0.5156(\pm0.0004)$
r_1(side)	$0.5711(\pm0.0019)$	$0.5700(\pm0.0006)$
r_1(back)	$0.5962(\pm0.0023)$	$0.5947(\pm0.0007)$
r_2(pole)	$0.2335(\pm0.0015)$	$0.2326(\pm0.0004)$
r_2(side)	$0.2506(\pm0.0018)$	$0.2440(\pm0.0005)$
r_2(back)	$0.2960(\pm0.0043)$	$0.2934(\pm0.0013)$
$\Sigma(O-C)_i^2$	0.2817	0.2624

5 DISCUSSION AND CONCLUSIONS

The photometric solutions were deduced from two sets of BVR light curves, indicating that EF Dra is a triple star system with a high fill-out factor. Combining the photometric solution (Sol.2) and spectroscopic elements (Lu & Rucinski 1999), the absolute physical parameters can be updated as follows: $a = 3.045(\pm0.028)\,R_\odot$, $M_1 = 1.815(\pm0.032)\,M_\odot$, $M_2 = 0.290(\pm0.026)\,M_\odot$, $R_1 = 1.702(\pm0.002)\,R_\odot$, $R_2 = 0.777(\pm0.002)\,R_\odot$, $L_1 = 3.961(\pm0.008)\,L_\odot$ and $L_2 = 0.793(\pm0.004)\,L_\odot$. The $O-C$ curve shows its orbital period may change in a complicated mode, i.e. a secular period increase superimposed with a light-time orbit. This kind of period variation may appear in other deep-contact binaries, whose spectroscopic parameters are listed in Table 6. From

Table 6 Parameters of Some Deep-contact Binaries with a Period Increase and a Cyclic Variation

Star	Period (d)	q	f (%)	dP/dt ($\times 10^{-7}$ d yr^{-1})	A (d)	$P_{\rm mod}$ (yr)	Ref.
XY Boo	0.3706	0.186	55.9	+6.54	0.0045	30.4	[1]
RR Cen	0.6057	0.205	35.1	+1.21	0.0124	60.1	[2]
AH Cnc	0.3604	0.168	58.5	+3.99	0.0237	36.5	[3]
V1191 Cyg	0.3134	0.107	68.6	+4.5	0.023	26.7	[4]
EF Dra	0.4240	0.160	46.7	+3.72	0.0038	17.2	[5]
V345 Gem	0.2748	0.142	72.9	+0.12	0.0019	1.77	[6]
BB Peg	0.3440	0.149	95.3	+0.30	0.0055	27.9	[7]
EM Psc	0.3440	0.149	95.3	+39.7	0.0110	3.3	[8]

References: [1] Yang (2006); [2] Yang et al. (2005); [3] Qian et al. (2006); [4] Zhu et al. (2011); [5] Present work; [6] Yang et al. (2010); [7] Kalomeni et al. (2007); [8] Qian et al. (2008).

this table, the period increase rate is a typical value. The semi-amplitude and period of the light-time orbit are smaller values.

5.1 Light-time Effect due to the Third Body

From Equation (3), the period and semi-amplitude of the light-time orbit are $P_{\rm mod} = 17.20(\pm 0.18)$ yr and $A = 0.0039^{\rm d}(\pm 0.0002^{\rm d})$, respectively. The existence of the tertiary component of EF Dra has been identified by the photometry and spectroscopy. From the fitted parameters of Equation (3), we can easily calculate the value of $a_{12}\sin i = 0.6752(\pm 0.0346)$ AU, where a_{12} and j are the radius and inclination of the orbit of the third body around the mass center of the binary system. Using the known equation,

$$f(m) = \frac{4\pi^2}{GP_{\rm mod}^2} \times (a_{12}\sin i)^3 = \frac{(M_3 \sin i)^3}{(M_1 + M_2 + M_3)^2}, \tag{4}$$

the mass function of $f(m) = 1.04(\pm 0.16) \times 10^{-3}\, M_\odot$ for the third body was computed. Therefore, for some orbital inclination i, the unknown mass M_3 can be derived by the iteration method. With the absolute parameters of EF Dra, the relations between the orbital inclination i, radii a_{12} and mass M_3 for the third body are displayed in Figure 4. According to the photometric solution, the value of L_3/L_1 is about 0.018. The visual magnitude of EF Dra is 4.0$^{\rm m}$, which is based on its spectral type of F8V (Cox 2000). Therefore, the value of the tertiary companion approximates $M_{\rm v} = 8.56^{\rm m}$, corresponding to a spectral type of K9 and a mass of $0.54\, M_\odot$. From Equation (4), we can deduce the orbital radius and inclination for the third component, i.e. $i = 21.0°(\pm 1.1°)$ and $a_{12} = 7.33(\pm 0.38)$ AU, which are shown as solid circles in both panels of Figure 4. Using the Harrington (1977) sufficient condition for the stability of a triple system, EF Dra should be dynamically stable.

5.2 Mass Transfer and Its Evolutionary Status

According to the binary-star evolution code (i.e. BSE; Hurley et al. 2002), we constructed the zero-age main sequence (ZAMS) and the terminal-age main sequence (TAMS) in a $\log L - \log M$ diagram in Figure 5, where the open circles and triangles represent the primary and the secondary of the A-type low-temperature contact binary systems (Yakut & Eggleton 2005). From this figure, it is found that the more massive component is close to the TAMS line, indicating that the primary component may be a normal main-sequence star. Moreover, the less massive component lies upon the TAMS line. This may be due to the energy transferring from the more massive component to the less massive one during its evolutionary process. Therefore, the secondary component is overluminous.

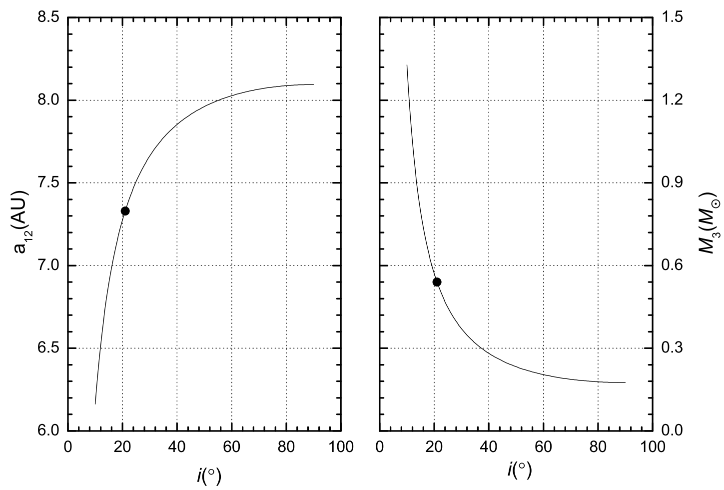

Fig. 4 Relations between the inclination i and radius a_{12} and mass M_3 for the third body from Eq. (4). The filled circles in both panels represent the positions of the third body, whose spectral type is $K9$, estimated from the third light of the photometric solution.

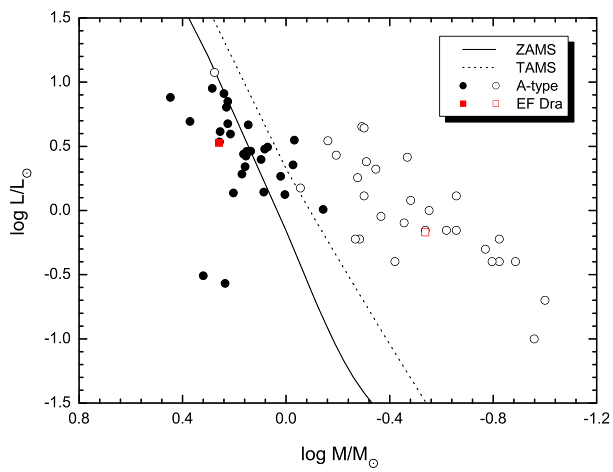

Fig. 5 Mass-luminosity diagram of the triple star system EF Dra. The open and filled circles refer to the primary and secondary components for the A-type low-temperature contact binaries (Yakut & Eggleton 2005). The solid and dotted lines show the ZAMS and TAMS lines, constructed by the *BSE* Code (Hurley et al. 2002).

From Equation (2), the orbital period of EF Dra increases at a rate of $dP/dt = +3.72(\pm 0.07) \times 10^{-7}$ d yr^{-1}, indicating that the mass transfers from the less massive component to the more massive one. Assuming there is conserved mass transfer, its rate can be estimated using the following equation (Singh & Chaubey 1986),

$$\frac{\dot{P}}{P} = 3\frac{1-q}{q}\frac{\dot{M}_1}{M_1}\,, \tag{5}$$

where M_1 and $\dot{M}_1$ are the mass of the primary component and its mass transfer rate, respectively. Inserting the values of $\dot{P}$, P, M_1 and q of EF Dra into Equation (5), the mass transfer rate can be estimated to be $\dot{M}_1 = +1.01(\pm 0.02) \times 10^{-7} M_\odot \text{ yr}^{-1}$. This situation occurs in other deep-contact binaries, listed in Table 6. With the period continuously increasing, the orbital angular momentum decreases while the spin angular momentum increases. Meanwhile, the separation between both components may increase, which may cause the contact degree to decrease. Moreover, a tertiary companion may remove angular momentum from the central system via a Kozai (1962) oscillation or a combination of a Kozai cycle and tidal friction (e.g., Fabrycky & Tremaine 2007), which may play an important role for the formation and evolution of the contact binary. For this kind of deep-contact binary, instability occurs when it meets the more familiar criterion that the orbital angular momentum is less than three times the total spin angular momentum (Hut 1980). Only if the contact configuration does not break down at $J_{\rm orb} > 3J_{\rm spin}$ could EF Dra merge into a rapidly rotating single star. In our future work, it is necessary for us to obtain high-precision eclipsing times in order to check the nature of its orbital period changes.

Acknowledgements This work was partly supported by the National Natural Science Foundation of China (Nos. 10778707 and 11133007)), Anhui Provincial Natural Science Foundation (No. 1208085MA04) and the Open Research Program (No. OP 201110) of the Key Laboratory for the Structure and Evolution of Celestial Objects of CAS. The author thanks Professor J.-M. Kreiner for sending his collected light minimum times of EF Dra. New observations of this binary were observed using the 60-cm telescope and the 85-cm telescope at the Xinglong Station of NAOC.

References

Agerer, F., Dahm, M., & Hübscher, J. 2001, Information Bulletin on Variable Stars, 5017, 1
Agerer, F., & Hübscher, J. 1995, Information Bulletin on Variable Stars, 4222, 1
Agerer, F., & Hübscher, J. 1996, Information Bulletin on Variable Stars, 4383, 1
Agerer, F., & Hübscher, J. 1997, Information Bulletin on Variable Stars, 4472, 1
Agerer, F., & Hübscher, J. 1999, Information Bulletin on Variable Stars, 4711, 1
Agerer, F., & Hübscher, J. 2002, Information Bulletin on Variable Stars, 5296, 1
Agerer, F., & Hübscher, J. 2003, Information Bulletin on Variable Stars, 5484, 1
Bate, M. R. 2004, in Revista Mexicana de Astronomia y Astrofisica Conference Series 21, eds. C. Allen, & C. Scarfe, 175
Borkovits, T., van Cauteren, P., Lampens, P., et al. 2008, Information Bulletin on Variable Stars, 5835, 1
Brát, L., Zejda, M., & Svoboda, P. 2007, Open European Journal on Variable Stars, 74, 1
Cox, A. N. 2000, Allen's Astrophysical Quantities (4th edn.)(New York: Springer)
Diethelm, R. 2001, BBSAG Bull., 125 (*http://www.calsky.com/?&bbsag=&sub3*)
Diethelm, R. 2002, BBSAG Bull., 128 (*http://www.calsky.com/?&bbsag=&sub=3*)
Diethelm, R. 2003, Information Bulletin on Variable Stars, 5438, 1
Diethelm, R. 2010, Information Bulletin on Variable Stars, 5945, 1
Drozdz, M., & Ogloza, W. 2005, Information Bulletin on Variable Stars, 5623, 1
Duerbeck, H. W., & Rucinski, S. M. 2007, AJ, 133, 169
Fabrycky, D., & Tremaine, S. 2007, ApJ, 669, 1298
Fleming, T. A., Gioia, I. M., & Maccacaro, T. 1989, AJ, 98, 692
Gioia, I. M., Maccacaro, T., & Wolter, A. 1987, in IAU Symp. 124, Observational Cosmology, eds. A. Hewitt, G. Burbidge, & L. Z. Fang, 593
Harrington, R. S. 1977, Revista Mexicana de Astronomia y Astrofisica, 3, 139
Hübscher, J. 2005, Information Bulletin on Variable Stars, 5643, 1
Hübscher, J., Agerer, F., Frank, P., & Wunder, E. 1994, Berliner Arbeitsgemeinschaft fuer Veraenderliche Sterne - Mitteilungen, 68, 1

Hübscher, J., Agerer, F., & Wunder, E. 1992, Berliner Arbeitsgemeinschaft fuer Veraenderliche Sterne - Mitteilungen, 60, 1
Hübscher, J., Agerer, F., & Wunder, E. 1993, Berliner Arbeitsgemeinschaft fuer Veraenderliche Sterne - Mitteilungen, 62, 1
Hübscher, J., Lehmann, P. B., Monninger, G., Steinbach, H.-M., & Walter, F. 2010, Information Bulletin on Variable Stars, 5918, 1
Hurley, J. R., Tout, C. A., & Pols, O. R. 2002, MNRAS, 329, 897
Hut, P. 1980, A&A, 92, 167
Irwin, J. B. 1952, ApJ, 116, 218
Kalomeni, B., Yakut, K., Keskin, V., et al. 2007, AJ, 134, 642
Kazarovets, E. V., & Samus, N. N. 1990, Information Bulletin on Variable Stars, 3530, 1
Kondo, Y., McCluskey, G. E., & Guinan, E. F. 2002, New Astron. Rev., 46, 1
Kozai, Y. 1962, AJ, 67, 579
Kreiner, J. M. 2004, Acta Astronomica, 54, 207
Kurucz, R. L. 1993, in Astronomical Society of the Pacific Conference Series 44, Peculiar versus Normal Phenomena in A-type and Related Stars, eds. M. M. Dworetsky, F. Castelli, & R. Faraggiana (San Francisco, CA: ASP), 87
Kwee, K. K., & van Woerden, H. 1956, Bull. Astron. Inst. Netherlands, 12, 327
Lu, W. 1993, Information Bulletin on Variable Stars, 3947, 1
Lu, W., & Rucinski, S. M. 1999, AJ, 118, 515
Lucy, L. B. 1967, ZAp, 65, 89
Molik, P. 2007, Open European Journal on Variable Stars, 60, 1
Nelson, R. H. 2006, Information Bulletin on Variable Stars, 5672, 1
Parimucha, S., Vanko, M., Pribulla, T., et al. 2007, Information Bulletin on Variable Stars, 5777, 1
Plewa, T., Haber, G., Wlodarczyk, K. J., & Krzesinski, J. 1991, Acta Astronomica, 41, 291
Press, W. H., Teukolsky, S. A., Vetterling, W. T., & Flannery, B. P. 1992, Numerical recipes in FORTRAN: The Art of Scientific Computing (Cambridge: Cambridge Univ. Press)
Pribulla, T., Baludansky, D., Chochol, D., et al. 2005, Information Bulletin on Variable Stars, 5668, 1
Pribulla, T., Rucinski, S. M., Blake, R. M., et al. 2009a, AJ, 137, 3655
Pribulla, T., Rucinski, S. M., Conidis, G., et al. 2007, AJ, 133, 1977
Pribulla, T., Rucinski, S. M., DeBond, H., et al. 2009b, AJ, 137, 3646
Pribulla, T., Rucinski, S. M., Lu, W., et al. 2006, AJ, 132, 769
Pribulla, T., Vanko, M., Chochol, D., & Parimucha, S. 2001a, Contributions of the Astronomical Observatory Skalnate Pleso, 31, 26
Pribulla, T., Vanko, M., Parimucha, S., & Chochol, D. 2001b, Information Bulletin on Variable Stars, 5056, 1
Pribulla, T., Vanko, M., Parimucha, S., & Chochol, D. 2002, Information Bulletin on Variable Stars, 5341, 1
Qian, S.-B., He, J.-J., Soonthornthum, B., et al. 2008, AJ, 136, 1940
Qian, S.-B., Liu, L., Soonthornthum, B., Zhu, L.-Y., & He, J.-J. 2006, AJ, 131, 3028
Robb, R. M., & Scarfe, C. D. 1989, Information Bulletin on Variable Stars, 3370, 1
Robertson, J. A., & Eggleton, P. P. 1977, MNRAS, 179, 359
Ruciński, S. M. 1973, Acta Astronomica, 23, 79
Rucinski, S. M., Capobianco, C. C., Lu, W., et al. 2003, AJ, 125, 3258
Rucinski, S. M., & Duerbeck, H. W. 2006, AJ, 132, 1539
Rucinski, S. M., Lu, W., Capobianco, C. C., et al. 2002, AJ, 124, 1738
Rucinski, S. M., Lu, W., Mochnacki, S. W., Ogłoza, W., & Stachowski, G. 2001, AJ, 122, 1974
Rucinski, S. M., & Pribulla, T. 2008, MNRAS, 388, 1831
Rucinski, S. M., Pribulla, T., Mochnacki, S. W., et al. 2008, AJ, 136, 586
Rucinski, S. M., Pych, W., Ogłoza, W., et al. 2005, AJ, 130, 767

Sarounova, L., & Wolf, M. 2005, Information Bulletin on Variable Stars, 5594, 1
Singh, M., & Chaubey, U. S. 1986, Ap&SS, 124, 389
Tohline, J. E. 2002, ARA&A, 40, 349
van Hamme, W. 1993, AJ, 106, 2096
Wilson, R. E. 1990, ApJ, 356, 613
Wilson, R. E., & Devinney, E. J. 1971, ApJ, 166, 605
Wunder, E., & Agerer, F. 1992, Information Bulletin on Variable Stars, 3811, 1
Yakut, K., & Eggleton, P. P. 2005, ApJ, 629, 1055
Yang, Y.-G. 2006, PhD thesis, Yunnan Observatory of Chinese Academy Sciences
Yang, Y.-G., Qian, S.-B., Zhu, L.-Y., He, J.-J., & Yuan, J.-Z. 2005, PASJ, 57, 983
Yang, Y.-G., Li, H.-L., Dai, H.-F., & Zhang, L.-Y. 2010, AJ, 140, 1687
Yang, Y.-G., Zhou, A.-Y., Dai, H.-F., & Yang, Y.-J. 2011, Information Bulletin on Variable Stars, 5998, 11
Zejda, M., Mikulasek, Z., & Wolf, M. 2006, Information Bulletin on Variable Stars, 5741, 1
Zhou, A.-Y., Jiang, X.-J., Zhang, Y.-P., & Wei, J.-Y. 2009, RAA (Research in Astronomy and Astrophysics), 9, 349
Zhu, L. Y., Qian, S. B., Soonthornthum, B., He, J. J., & Liu, L. 2011, AJ, 142, 124
Zinnecker, H., & Mathieu, R., 2001, in IAU Symp. 200, The Formation of Binary Stars (ASP Publ.)